Extraction in Thin Liquid Films Generated by Impinging Streams

Yuli Berman and Abraham Tamir
Dept. of Chemical Engineering, Ben-Gurion University of the Negev, Beer-Sheva 84105, Israel

A new device for liquid–liquid extraction was developed, tested, and modeled, based on two immiscible thin films, flowing one on the top of the other while exchanging mass. The films are formed by impinging streams: collision of two immiscible jets flowing one toward the other on the same axis. Thus, the flow of the films is in a direction perpendicular to the initial flow of the jets. Two liquid systems (diluent–solute–solvent) were tested: water–iodine–kerosene and aqueous solution of HCl–pure water. In the latter case, HCl is transferred from its initial solution comprising one film to the other film of pure water flowing on the top of it. The experiment determined geometrical parameters of the thin film, mass-transfer coefficients of the solute between the films, as well as power input. For a relatively identical power input, the measured mass-transfer coefficients were higher by a factor of 10–200 compared to conventional devices. In addition, the mean residence time in the new device is shorter than in conventional devices due to minimal dispersion of the phases during the extraction stage, making the settling stage relatively simple and short.

Introduction

Liquid–liquid extraction, a widespread process in the chemical industry, is a method for separating the components of a solution by their distribution between two immiscible, or partially miscible liquids. It has been used for recovering various organic and inorganic compounds from various solutions in the petroleum, pharmaceutical, metallurgical, nuclear, and other industries (Laddha and Degaleesan, 1976; Treyball, 1963; Kogan, 1977; Rydberg et al., 1992). In parallel, research on various extraction processes has also been continued (Czapla and Bart, 1998; Wilson and Manousiouthakis, 1998; Bouaifi and Roustan, 1998; Rauline et al., 1998; Angelov et al., 1998), as is that in biotechnology analyses (Weigl and Yager, 1999).

Various types of extraction devices have been used, such as spray towers, perforated plate columns, pulse columns, centrifugal extractors, and mixer-settlers (Laddha and Degaleesan, 1976; Treyball, 1963; Kogan, 1977; Rydberg et al., 1992). For any extraction process the total process time, t_{tot}, is of a particular importance, that is,

$$t_{\text{tot}} = t_m + t_s, \tag{1}$$

where t_m is the mixing and extraction time of a solute recovering from feed to solvent, while t_s is the time of phases separation in the settler. Generally, in order to reduce the size of the equipment for a given throughput, t_{tot} should be minimized. Shortening t_m may be achieved by increasing the surface area between the phases (Handlos, 1957; Laddha and Degaleesan, 1976; Treyball, 1963; Kogan, 1977; Ryberg et al., 1992; Brounshtein and Fishbein, 1977), which, on the other hand, will increase t_s. Thus, these conflicting effects become a serious restriction in modern design of extraction equipment. As shown in the following, the application of impinging streams for generating thin films that make up the major element of the new device, solves the preceding problem.

The first patent on method and apparatus for mixing and contacting fluids by impinging streams was probably obtained by Carver et al., (1956). It was found that the extraction efficiency of alcohol from water into kerosene attains a maximum of 96%. However, no mass-transfer coefficients or power input were reported. Additional methods for dispersing one liquid into the other (Janssen et al., 1993) make use of the stagnation flow of two opposed liquid jets forming hyperbolic flow streamlines, and the impinging-stream jet mixer (Treyball, 1963, p. 142).

Correspondence concerning this article should be addressed to A. Tamir.

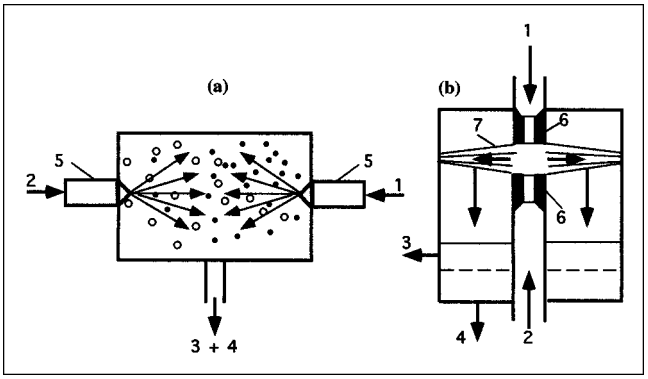

Figure 1. Principal schemes of extraction in impinging streams.

(a) In dispersion; (b) in thin films. 1—Initial solution; 2—solvent; 3—light phase; 4—heavy phase, 5—nozzles for liquid atomization; 6—coaxial nozzles; 7—two films flowing one on the top of the other.

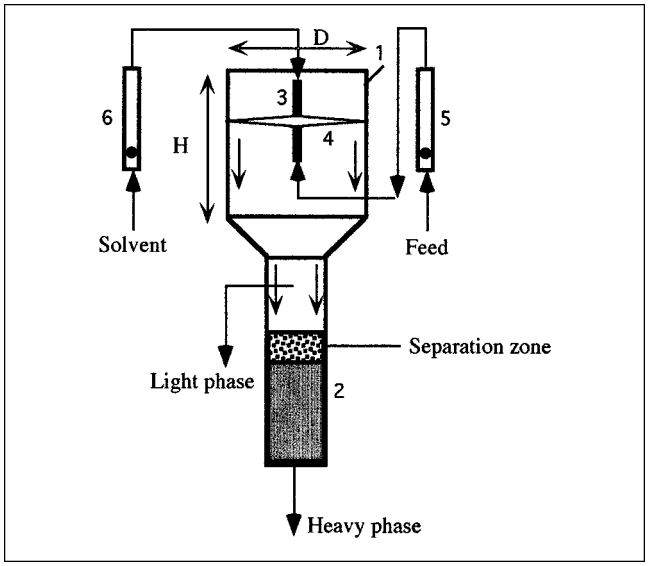

Figure 2. Laboratory setup for extraction in thin films.

A new device for liquid–liquid extraction based on impinging streams (Tamir, 1994), shown in Figure 1a, was developed in the past and tested in our laboratory. Feed 1 and solvent 2 are introduced into the system through spray nozzles 5 positioned one toward the other on the same axis, which caused atomization of the liquid at their exit. Mixing between the phases, intensive mass transfer due to a droplet's coalescence in the impact zone and on the walls of the reactor, as well as a relatively short contact time are achieved due to the impinging-stream configuration. Extraction experiments with the water–iodine–kerosene and kerosene–acetic acid–water (diluent–solute–solvent) systems indicated that the impinging-stream device yielded (Tamir, 1994, table 12-2) the highest volumetric mass-transfer coefficients, of the order of 0.001–0.3 s^{-1} as compared to regular devices for which the maximum coefficient was 0.03 s^{-1}. However, in the impinging-stream device, power input was relatively high, 35–1500 kJ/(m^3liquid), as compared to other devices (Tamir, 1994, table 12-3). The high-power input in the impinging stream was caused by creation of droplets with spray nozzles in order to achieve large mass-transfer areas, as well as other characteristics of impinging streams.

The major aim of the present investigation was to develop an extraction device exhibiting high mass-transfer coefficients at a relatively low input power, as well as model it for scale-up purposes. Figure 1b shows the essence of a new device in which two immiscible liquid streams, feed 1 and solvent 2, leave nozzles 6 in the form of cylindrical jets. The two jets collide at the impinging plane, forming thin films 7, of the order of 10–500 microns, which flow one on the top of the other in a plane perpendicular to the initial jets. Theoretical and experimental investigations indicated that the motion of the thin films is of a wavy turbulent character, which intensify the mass transfer (Kapiza, 1948; Davies, 1972; Taylor, 1960; Chu and Dukler, 1974; Hasson and Peck, 1964; Boyadjiev and Beshkov, 1984). Thus, the elimination of the formation of droplets and the application of extremely thin, wavy, and turbulent films, flowing one on the top of the other for solute recovery, as demonstrated in the present investigation, created a significant enhancement of the mass transfer between the phases, with relatively low power consumption. This reduces the mixing and extraction time t_m between the solvent and the solute in the feed. In addition, due to the flow of the films one on the top of the other, with minimal dispersion of the phases, their separation in the settler becomes relatively easy and fast, that is, t_s, the time of phases settling, is simultaneously shortened. Thus, t_{tot}, the overall extraction-settling time in Eq. 1 is reduced, manifesting the major advantage of the new device.

Experimental Studies

Setup

The impinging-stream scheme in Figure 1b for generating thin films of a circular shape flowing one on the top of the other, was realized in a laboratory setup made up of the single extractor-settler unit shown in Figure 2. It was manufactured of transparent Plexiglas for determining the diameter of the circular films by photography. The experimental system consisted of the following elements:

1. Reactor 1 of diameter $D = 0.11$, 0.15 m and height $H =$ 0.004–0.04 m, in which extraction takes place in the thin films 4.
2. Two coaxial nozzles 3 of diameter $(1–5)\times10^{-3}$ m. The clearance between the nozzles varied in the range of $(0.05–2)\times10^{-3}$m.
3. Settler 2 of diameter 0.04 m and height 0.15 m, in which separation of the phases into light and heavy takes place.
4. Rotameters 5, 6 for the feed and solvent.
5. Pumps for feed and solvent. In addition, manometers were installed for measuring pressure drop on the nozzles to determine the power input.

Liquids tested

Two liquid systems (diluent–solute–solvent) were tested: (1) aqueous solution of HCl–pure water where all liquids are miscible; and (2) water–iodine–kerosene where water and

kerosene are immiscible. In the first case, a solution of HCl was introduced into one nozzle and pure water into the second nozzle. The extraction process was the transfer of HCl from the aqueous solution comprising one film into the other film of pure water flowing on top of it. The employment of this system made it possible to test the setup at relatively high stream flow rates. The second system was chosen due to the rapid change in the color of the phases, water and kerosene, when iodine was extracted by the kerosene. It should also be noted that another reason was a practical case in which iodine was extracted by kerosene from Chilean saltpeter by the SQM process (McKetta, 1984, p. 718). The solubility of iodine in water is usually very small. Thus, KI was added to the water, resulting in the following reaction $I_2 + I^- \rightarrow I_3^-$, which increased the solubility of the iodine in the form of the I_3^- complex. In addition, this complex can be easily determined (Manzurela, 1977).

Procedure and analyses

An experimental run consisted of the following procedure. Feed (HCl aqueous solution or iodine solution in water) and the solvent (pure water or kerosene, respectively) were fed into reactor 1 in Figure 2. At steady state, reached after 5–10 min, samples of the solution were taken at the inlet to reactor 1 and the exit of the thin films, that is, initial and final concentrations. The latter were determined by well-known titration methods. In the case of HCl, samples of 0.5 mL were taken directly from the edge of the film. This was done by carefully placing a small syringe's needle near the surface of the pure water side into which diffusion of HCl took place from the HCl aqueous solution film. It should be noted that in the absence of turbulence in the film, it is expected that the two initial films do not mix. In some cases, 25 samples of the final concentration were taken for determination of the statistical variance.

Experimental range

I. Aqueous solution of HCl–pure water: Initial concentration of HCl in water, $x_1 = (10–50)$ mg/mL; diameter of nozzles, $d_0 = (1–5)\times 10^{-3}$ m; clearance between nozzles, $\delta = (0.1–2)\times 10^{-3}$ m; flow rates of the liquids, Q_s and $Q_r = (2–20)\times 10^{-6}$ m^3/s; the ratio $\gamma = Q_s/Q_r = 1$; height of reactor, $H = 20\times 10^{-3}$ m.

II. Water–iodine–kerosene: Initial concentration of iodine in water, $x_1 = (0.2–0.5)$ mg/mL; diameter of nozzles, $d_0 = 1\times 10^{-3}$ m; clearance between nozzles, $\delta = (0.05–0.5)\times 10^{-3}$ m; flow rates of the liquids, Q_s and $Q_r = (3–10)\times 10^{-6}$ m^3/s; the ratio $\gamma = Q_s/Q_r = 0.2–2.5$; height of reactor, $H = (4–40)\times 10^{-3}$ m. The experimental error was $\pm$10–15%.

Modeling, Results, and Discussion

Phases-separation rate

The phase-separation rate in the settler (2 in Figure 2) was determined as the rate at which the dispersion zone of the phase disappears after the liquid flow into the reactor was terminated (Marchuk, 1980). Experiments were conducted with the water–iodine–kerosene system, for which the height of the dispersion zone was $(10–20)\times 10^{-3}$ m and the mean separation rate about 20×10^{-3} m/s. The settler's effectiveness was determined by comparing its separation rate with that of a laboratory agitated vessel of 0.10 m diameter and height of 0.15 m, in which a water–iodine–kerosene solution with volumetric ratio of water to kerosene of 0.5–1 was intensively mixed. The optimal mean residence time of the liquids in the vessel was about 60 s, the initial height of the separation zone $(100–120)\times 10^{-3}$ m, and the average separation rate was about 2×10^{-3} m/s. As seen, the separation rate in the new thin liquid film device was about 10 times higher compared to the agitated vessel. This is probably due to the minimal dispersion between the thin films.

Geometry of the thin film

Figure 3 shows the formation of the thin film. Two immiscible liquid streams, feed and solvent, leave the nozzles, 1, with clearance δ between them in the form of cylindrical jets. The two jets collide at the impinging plane, forming extremely thin films of varying thickness, h, with initial thickness of the order of 100–500 micron. These films flow one on top of the other in a plane perpendicular to the initial jets. The initial thickness of the film is L ($> h$), and its average radius is R, where $R/r_0 > 1$. Two cases are demonstrated in Figure 3: $\delta \geq r_0$ and $\delta < r_0$, for which appropriate relationships, Eqs. 6a and 6b, are derived below, where if $\delta < r_0$, then $L = \delta$, and if $\delta \geq r_0$, then $L = r_0$. The latter result follows from Eq. 4 because the velocity vector only changes its direction by 90° and not its magnitude, namely $u_0 = u_n$. As shown later, the basic parameters that affect the mass transfer in the film are its thickness and radius. Thus, in the following, these quantities will be considered from the theoretical point of view.

In general, gravity, viscosity, and friction with the air are the forces that may affect the motion in the film. However, evaluation of the effect of these forces, considering the relative high velocity in the film, $u_0 > 1$ m/s, indicated that their effect can be ignored. Therefore, it can be assumed (Taylor, 1960; Hasson, 1964; Ranz, 1959) that the liquid motion in the film is inertial; thus, its average velocity u_0 remains constant.

Conservation of the momentum rate between the beginning of the film near the exit from the nozzles and any point along its thickness h in Figure 3 reads

$$\rho u_0^2 L 2\pi r_0 = \rho u_0^2 h 2\pi R, \qquad (2)$$

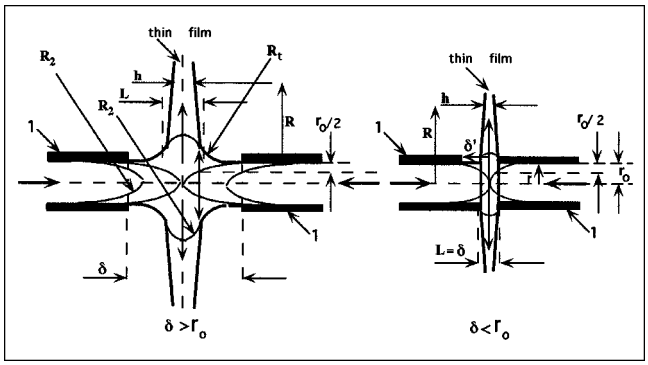

Figure 3. Formation of the thin film by impinging streams.

yielding the local film thickness:

$$h = Lr_0/R \quad \text{or} \quad h/L = r_0/R. \tag{3}$$

Conservation of mass between the exit of the nozzles and the beginning of the film reads

$$\rho 2\pi r_0 L u_0 = \rho 2\pi r_0^2 u_n, \tag{4}$$

yielding that

$$u_0/u_n = r_0/L. \tag{5}$$

Two cases are considered with respect to Figure 3:

1. $\delta \geq r_0$ resulting in

$$u_0/u_n = 1 \quad \text{and} \quad L = r_0, \tag{6a}$$

which is also applicable for conditions of a free-flowing film.

2. $\delta < r_0$ yielding $\delta = L$, so,

$$u_0/u_n = r_0/\delta > 1. \tag{6b}$$

Combining Eqs. 3 and 6a results in the following equation for the free-flowing film, also obtained in Ranz (1959) and Hasson (1964):

$$hR/r_0^2 = 1. \tag{7}$$

For a continuous film, a balance between inertia and surface tension forces (Millikan et al., 1965) yields the following equation for the maximum radius of the film:

$$\rho u_0^2 h 2\pi R = 4\pi R^2 \sigma \left(\frac{1}{R} + \frac{1}{R_2}\right) = \frac{4\pi R^2 \sigma}{R}\left(1 + \frac{R}{R_2}\right). \tag{8}$$

Combining Eqs. 8 and 3 yields

$$\frac{R}{r_0} = \frac{L\rho u_0^2}{2\sigma[1 + R/R_2]}. \tag{9}$$

If $L = r_0$ and $R_2 \to \infty$, that is, the external surface of the film thickness is plain, it follows from Eq. 9 that

$$\frac{R}{r_0} = \frac{r_0 \rho u_0^2}{2\sigma}. \tag{10}$$

Ranz (1959) wrote that Eq. 10 gave large deviations for small nozzles, due to flow disturbances inside the nozzle, and for the large nozzles, due to the effects of gravity. Comparison between calculations based on Eq. 10 and experimental data of Kawada (Ranz, 1959) indicated that these data were lower by a factor of nearly $3^{1/2}$. Similarly, our experimental data were 2–3 times lower than those predicted by Eq. 10. Thus, the surface curvature of the film edge related to the term $[1 + R/R_2]$ in Eq. 9 affects the results and will be determined in the following. It is now assumed that

$$R/R_2 = (R/R_2)_{R = r_0} = \text{constant}. \tag{11}$$

Table 1. Experimental vs. Calculated Values of R/r_0 for the System Water–HCl–water

u_o (m/s)	R/r_o Exp.	R/r_o Calc.	Dev. %	u_o (m/s)	R/r_o Exp.	R/r_o Calc.	Dev. %
Case 1				*Case 2*			
1.66	6.5	5.7	−12.9	1.0	4.0	3.8	−5.3
1.90	7.5	7.4	−1	1.1	4.0	4.9	22.0
2.07	8.0	8.8	10	1.24	7.1	6.2	−12.9
2.30	9.0	10.9	21	1.33	7.8	7.1	−8.5
2.55	11.5	13.3	15.6	1.37	8.2	7.6	−8.0
2.71	14	15.0	7.4	1.53	10.2	9.4	−7.7
2.87	15	16.9	12.9	1.62	10.7	10.6	−1.1
3.11	17.5	19.9	13.7	1.76	12.4	12.5	0.3
3.19	19	20.8	9.5	1.96	12.9	15.5	20.0
3.27	21.5	22.0	2.3	2.50	26.5	25.2	−4.9

1. $L/r_0 = 1$, $r_0 = 10^{-3}$m, $Re \leq 1{,}650$; 2. $L/r_0 = 0.44$, $r_0 = 2.55 \times 10^{-3}$m and $Re_{\max} = 5{,}600$.
Abbreviations: Exp.—experimental; Calc.—calculated; Dev.—deviation.

This assumption, as well as the following definition in Eq. 13, which yields Eq. 19, is justified by the satisfactory agreement between experimental results and the theoretical predictions given in Table 1. In addition, Figure 3 indicates that the velocity vector changes its direction by 90° after collision and formation of the sheet (Elperin, 1972; Tamir, 1994; Popiel and Tass, 1991). Thus, it is further assumed that as soon as the flow begins in the thin film, the following conditions hold for its initial velocity profile, assuming also that liquid average velocity equals u_0 in the nozzles:

1. $L = r_o$

$$\begin{aligned} &\delta' = 0: \quad u = u_{r=o}\,(\text{nozzle}) = u_{\max}\,(\text{nozzle}) \\ &\delta' = L/2: \quad u = u_{r=r_o/2}\,(\text{nozzle}). \end{aligned} \tag{12a}$$

2. $L < r_o$

$$\begin{aligned} &\delta' = 0: \quad u = u_{r=r_{o,\text{eq}}=0} = u_{\max}\,(\text{equivalent nozzle}) \\ &\delta' = L/2: \quad u = u_{r=r_{o,\text{eq}}/2}\,(\text{equivalent nozzle}). \end{aligned} \tag{12b}$$

As noted, an equivalent radius $r_{o,\text{eq}}$ was defined on the basis of the following mass balance

$$\rho\pi r_o^2 u_n = \rho\pi r_{o,\text{eq}}^2 u_o, \tag{13}$$

yielding

$$r_{o,\text{eq}}/r_o = (u_n/u_o)^{0.5}. \tag{14}$$

An expression for R_2 was suggested elsewhere (Korn and Korn, 1968) in a dimensionless form $y^* = R_2/(L/2)$; it reads

$$y^* = \left[1 + \left(\frac{dZ}{dX}\right)^2\right]^{3/2} \Bigg/ \left[\frac{d^2 Z}{dX^2}\right] = F(X), \tag{15}$$

where

$$Z = u/u_{\max} = f(X) \quad \text{and} \quad X = r/r_o \qquad (0 \leq X \leq 0.5) \tag{15a}$$

The dimensionless mean value of $\bar{y}^*$ is given by

$$\bar{y}^* = (1/0.5)\int_0^{0.5} y^*\, dX, \tag{16}$$

where

$$\bar{y}^* = \bar{R}_2/(L/2). \tag{16a}$$

From the preceding definition it follows that

$$\left(\frac{R}{\bar{R}_2}\right)_{R=r_o} = \frac{2r_o}{\bar{y}^* L}, \tag{17}$$

where Eq. 6a for $1 \geq r_o$ yields

$$\left(\frac{R}{\bar{R}_2}\right)_{R=r_o} = \frac{2}{\bar{y}^*}. \tag{18a}$$

On the other hand, for $\delta < r_o$ it follows that $L = r_{o,\mathrm{eq}}$, and according to Eq. 14,

$$\left(\frac{R}{\bar{R}_2}\right)_{R=r_o} = \frac{2}{\bar{y}^*}\left(\frac{u_o}{u_n}\right)^{0.5}. \tag{18b}$$

Thus, Eq. 9 yields

$$\frac{R}{r_o} = \frac{L\rho u_o^2}{2\sigma\left[1+\frac{2}{\bar{y}^*}\left(\frac{u_o}{u_n}\right)^{0.5}\right]}. \tag{19}$$

Equations 15 and 16 make it possible to calculate the dimensionless radius of curvature of the film, $\bar{y}^*$, once the velocity is known; for example:

1. For turbulent flow the velocity profile is approximately flat, that is, $Z = 1$, thus $\bar{y}^* \to \infty$ and R/r_o is given by Eq. 10.
2. For laminar flow $Z = 1 - X^2$ and according to Eqs. 15 and 16, for the initial velocity profile in the film, $X = 0$ and $X = 0.5$, yielding that Z varies between 1 and 0.75. Thus, the mean value of y^* reads $\bar{y}^* = 1/0.5\int_0^{0.5} y^*\, dX = 0.86$.
3. For other cases where the velocity profile is not described explicitly, $\bar{y}^*$ is calculated from Eq. 19 on the basis of experimental data of R/r_o and other needed data. For the water–iodine–kerosene systems and aqueous solutions of HCl–pure water (Figure 4). As seen, $\bar{y}^*$ increases by decreasing L/r_o, where u_o increases according to Eq. 5, while the velocity profile becomes flatter. It is important to emphasize that if the values of $\bar{y}^*$ are calculated on the basis of experimental data (R/r_o, u_o, and σ) by Eq. 19 for laminar flow inside the nozzle ($Re < 2{,}300$), it is found that $\bar{y}^* = 0.86$; the latter coincides with the theoretical value obtained by the integral given earlier.

Table 1 reports experimental results for a water film in which mass transfer of HCl, reported in the following, also takes place. As observed, there is satisfactory agreement between the experimental and calculated results. It should be noted that if the physical properties of the components are significantly different from each other, the following mean values of the density and surface tension, respectively, are applied:

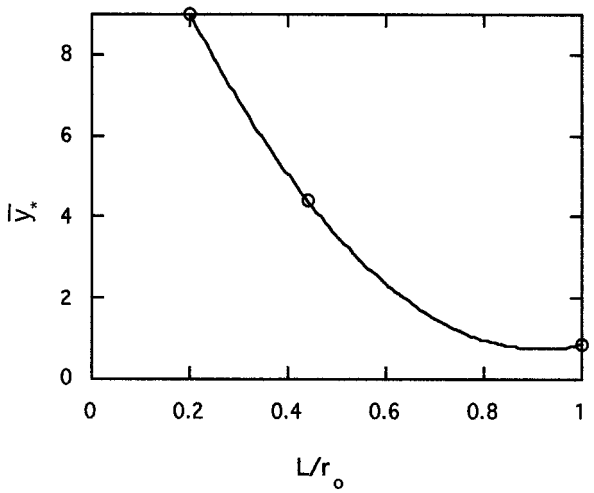

Figure 4. Dimensionless radius of curvature of the film vs. dimensionless initial film thickness for HCl–water jets ($R_c^2 = 0.99$).

$$\bar{\rho} = (\rho_r + \gamma\rho_s)/(1+\gamma) \qquad \bar{\sigma} = (\sigma_r + \gamma\sigma_s)/(1+\gamma), \tag{20}$$

where ρ_r and ρ_s and σ_r and σ_s are, respectively, the densities and the surface tensions of the pure raffinate and solvent, respectively, and γ is defined by Eq. 27.

Kinetics of the mass transfer

One of the basic characteristics of any transfer process is the mass-transfer coefficient k'(m/s). However, its determination in the present investigation is not possible because the exact surface area between the phases in the film is not known due to its wavy and turbulent nature. Therefore, the mass-transfer coefficient k(m/s) given in Eq. 26 with respect to the geometrical area will be applied.

Usually, the modeling starts with the following mass balances (Laddha and Degaleesan, 1976; Treyball, 1963; Kogan, 1977) in the raffinate (feed) and solvent (extract), respectively:

$$Q_r(x_1 - x_2) = k_r' S\Delta\bar{x} \tag{21}$$

$$Q_s(y_2 - y_1) = k_s' S\Delta\bar{y}, \tag{22}$$

where

$$\Delta\bar{x} = \frac{(x_1 - x_1^*) - (x_2 - x_2^*)}{\ln\dfrac{x_1 - x_1^*}{x_2 - x_2^*}} \tag{23}$$

$$\Delta\bar{y} = \frac{(y_1^* - y_1) - (y_2^* - y_2)}{\ln\dfrac{y_1^* - y_1}{y_2^* - y_2}}. \tag{24}$$

Since the actual surface area, S, for the mass transfer between the raffinate and solvent is not known, the following ratio is defined

$$C = S/(\pi R^2), \tag{25}$$

that is, C is the ratio between the actual area and the geometrical area for the mass transfer between the phases. $C > 1$ corresponds to a wavy and turbulent film (Kapiza, 1948; Davies, 1972; Taylor, 1960; Chu and Dukler, 1974; Hasson, 1964; Boyadjiev and Boshkov, 1984) or for phase dispersion; $C < 1$ indicates that the geometrical surface area has not been fully utilized. Considering Eqs. 21 and 22 leads to the following modified definition of the mass-transfer coefficients with respect to the geometrical area;

$$k_r = Ck'_r \qquad k_s = Ck'_s. \tag{26}$$

Making the following definition

$$\gamma = Q_s/Q_r \tag{27}$$

yields that

$$Q_{\text{tot}} = Q_r + Q_s + Q_{\text{sol}} \cong Q_s(1+\gamma)/\gamma = Q_r(1+\gamma) = 2\pi r_0 L u_0 \tag{28}$$

$$(x_1 - x_2)/(y_2 - y_1) = \gamma, \tag{29}$$

where the flow rate of the solute Q_{sol} is negligible. Applying the preceding quantities yields the following nondimensional numbers resulting from Eqs. 21–24:

$$N_r = \frac{k_r \pi R^2}{Q_{\text{tot}}} = \frac{1}{1+\gamma}\left[\frac{\ln\dfrac{x_1 - x_1^*}{x_2 - x_2^*}}{1 + \dfrac{x_2^* - x_1^*}{x_1 - x_2}}\right] \tag{30}$$

$$N_s = \frac{k_s \pi R^2}{Q_{\text{tot}}} = \frac{\gamma}{1+\gamma}\left[\frac{\ln\dfrac{y_1^* - y_1}{y_2^* - y_2}}{1 + \dfrac{y_1^* - y_2^*}{y_2 - y_1}}\right]. \tag{31}$$

The quantities N_r and N_s, considering Eq. 28, can be expressed as a function of the hydrodynamic conditions, Re, as well as physical properties, Sc, and in the present case also as a function of φ, as follows:

$$N_r = Sh_r/(2\,ReSc_r\varphi) \quad \text{and} \quad N_s = Sh_s/(2\,ReSc_s\varphi), \tag{32}$$

while the following definitions are applicable:

$$Re = u_0 R/\bar{\nu}; \qquad \varphi = h/R = r_0 L/R^2 = Q_{\text{tot}}/(2\pi u_0 R^2);$$
$$Sh_i = k_i R/D_i; \qquad Sc_i = \nu_i/D_i, \tag{33}$$

where $i = r$ for raffinate and $i = s$ for solvent; and $\bar{\nu}$ is the mean kinematic viscosity of the film. It should be noted that the righthand sides of Eqs. 30 and 31 are a function of the experimental conditions, that is, flow rates as well as initial and final concentrations of the solute in the raffinate and solvent. In addition the following relationships, which are determined from the experimental equilibrium curve, are applicable using Eq. 29:

$$x_1^* = f(y_1); \qquad x_2^* = f(y_2) = f\left[y_1 + (x_1 - x_2)/\gamma\right]$$
$$y_1^* = f(x_1); \qquad y_2^* = f(x_2) = f\left[x_1 - (y_2 - y_1)\gamma\right]. \tag{34}$$

If the equilibrium curve is a straight line, $f = m$, where m is the coefficient of distribution of the solute between the phases. In this case, Eqs. 30 and 31 will be written in the usual form for extraction processes (Treyball, 1963, p. 403, table 10.1).

Equations 30 and 31 also indicate, on the basis of experimental data, that it is possible to determine the mass-transfer coefficients. In addition, the following efficiencies indicating the degree of approach of the process toward equilibrium conditions can be determined:

$$E_{Mr}(\%) = 100\frac{x_1 - x_2}{x_1 - x_2^*} \qquad \text{and} \qquad E_{Me}(\%) = 100\frac{y_2 - y_1}{y_2^* - y_1} \tag{35}$$

Additional important quantities are the volumetric mass-transfer coefficient $K(\text{s}^{-1})$ defined below assuming that the volume of the reactor is given by $V_r = \pi R^2 H$:

$$K_r = \frac{k_r \pi R^2}{V_r} = \frac{k_r}{H} \qquad \text{and} \qquad K_s = \frac{k_s \pi R^2}{V_r} = \frac{k_s}{H}, \tag{36}$$

as well as the liquid mean residence time in the reactor, $\bar{t}$, which reads

$$\bar{t} = \frac{V}{Q_{\text{tot}}} \cong \frac{R}{u_0}. \tag{37}$$

The experimental work consisted of determining the extraction efficiencies as well as mass-transfer coefficients as functions of the operating conditions. Preliminary experiments were conducted to determine the effect of the ratio H/r_0. It has been established that for $H/r_0 \geq 8$ and a constant value of u_0, the extraction efficiency given by Eq. 35 and the mass-transfer coefficient remain practically unchanged. For the water–iodine–kerosene system the results shown in Table 2 were obtained. The behavior of these results can be explained as follows. The thin film demonstrates a wavy behavior that intensifies the mass transfer; the amplitude of the waviness is on the order of the average film thickness or less (Chu and Vuklar, 1974). Thus, there is a minimal H below which the effect of the waviness is eliminated, while it is effective above this value. In the present case, minimal H is approximately $4 \cdot 10^{-3}$ m.

Figure 5a and 5b demonstrate the results of extraction efficiencies, E_{Me} and E_{Mr}, against the average liquid film velocity u_0. As observed, the efficiencies are independent of the initial concentration of HCl and of the ratio $\gamma = Q_s/Q_r$, but,

Table 2. Effect of Reactor's Height H on E_{Mr} for $r_0 = 0.5 \times 10^{-3}$ m

$H \times 10^3 (m)$	4	10	15	20	40	Means
E_{Mr}(%) for $L = 0.1 \times 10^{-3}$ m and $u_0 = 19$ m/s	91.3	95	93.1	91	92	92.5
Deviation (%)	−1.3	2.7	0.6	−1.6	−0.5	
E_{Mr}(%) for $L = 0.3 \times 10^{-3}$ m and $u_0 = 6.4$ m/s	48.7	—	49	—	52	50
Deviation (%)	−2.6	—	−2	—	4	

Deviations are in the range of experimental error.

as expected, are increasing by increasing the velocity u_0, which strongly depends on the chemical system. For achieving an efficiency of 98%, u_0 is approximately 2 m/s for water–HCl–water, and 30 m/s for water–iodine–kerosene.

Mass-transfer coefficients were computed as follows. For the water–HCl–water system, the distribution coefficient between the phases is $m = 1$ and, correspondingly, $N_s = N_r$ and $k_r = k_s$; thus, Eq. 31 reads (Treyball, 1963, table 10.1):

$$k_r = k_s = -\frac{Q_{\text{tot}}}{\pi R^2} \frac{\gamma}{(1+\gamma)^2} \ln\left[1 - \frac{(1+\gamma) E_{Me}}{\gamma + E_{Me}}\right] \quad (38)$$

where $R = f(u_0)$ as demonstrated by Eq. 19. The following equation was obtained for the equilibrium curve for the water–iodine–kerosene system:

$$y_2^* = x_2^{0.615} \qquad x_2^* = y_2^{1.626}.$$

Since the curve is nonlinear, Eq. 30 was applied for computing k_r. The experimental mass-transfer coefficients varied in the range of 4×10^{-3}–73×10^{-3} m/s for the aqueous solution of HCl–water, and 0.5×10^{-3}–2×10^{-3} m/s for water–iodine–kerosene. The data were correlated by the following equation:

$$Sh_i = A Re^{\alpha} Sc_i^{\beta} \left(\varphi \times 10^3\right)^{\theta}, \quad (39)$$

where all quantities were defined in Eq. 33. Physical data needed were $\nu = 1 \times 10^{-6}$ m^2/s for water and 5×10^{-6} m^2/s for kerosene (Kutateladze and Borishansky, 1959; Perry, 1950); $D_{\text{HCl-water}} = 2.64 \times 10^{-9}$ m^2/s (Perry, 1950); and $D_{I_3^-\text{-water}} \cong 0.35 \times 10^{-9}$ m^2/s (Reid et al., 1987). Under the experimental conditions, the film's Reynolds number varied in the range of 1.10^4–1×10^6, namely, turbulent flow. Under these conditions, various investigations (Treyball, 1963; Kogan, 1977; Brounshtein and Fishbein, 1977; Eckert and Drake, 1961) indicated that $\alpha = 0.8$–0.83 and $\beta = 0.33$–0.55, where similar results were also obtained in the present experiments: $\alpha = 0.83$ and $\beta = 0.5$.

The determination of A and θ in Eq. 39 was based on the data presented in Figure 6a and 6b, which depend on the ratio R/R_r. Values of $R/R_r = (R/r_0)\,(r_0/R_r)$ were obtained for $r_0/R_r = 0.5/50$, whereas R/r_0 was computed from Eq. 19 and $\bar{\rho}$ and $\bar{\sigma}$ from Eq. 20. It was found that when $R/R_r < 1$, R/r_0 vary in the range of 50–100, and when $R/R_r > 1$, R/r_0 vary in the range of 170–460. Analysis of the data presented in Figure 6a and 6b with respect to Eq. 39 indicated that under different conditions, $\theta = 0.67$. However, $A = 0.4$ for the water–HCl–water system, but for water–iodine–kerosene $A = 0.133$ for $R/R_r < 1$, and $A = 0.266$ for $R/R_r > 1$, where the higher value of A is caused by additional mixing of the film due to its impact on the walls of the reactor. In addition, the coefficient A, and consequently the mass-transfer coefficients, is dependent on the type of the chemical system where similar results were also reported elsewhere (Laddha and Degaleesan, 1976; Treyball, 1963). For example, extraction mass-transfer coefficients in the toluene–diethyl amine–water and kerosene–acetone–water systems differ by a factor of 2. Finally, it should be noted that the coefficient A and the exponents in Eq. 39 were obtained for the water–HCl–water and water–iodine–kerosene chemical systems. For a more complete discussion of the data, one should consider the list suggested by the European Federation of Chemical Engineering (Rydberg et al., 1992; Misek, 1987).

In the following we consider the case where $R/R_r \geq 1$. Under these conditions, the basic parameters affecting the mass

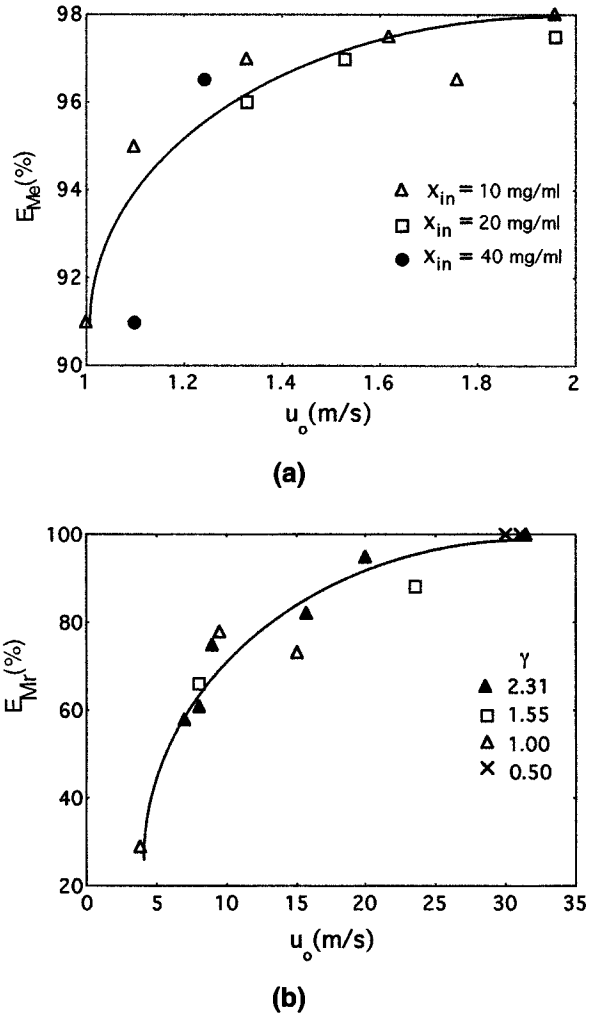

Figure 5. (a) Extract efficiency vs. film velocity for water–HCl–water ($R_c^2 = 0.90$), (b) raffinate efficiency vs. film velocity for water–iodine–kerosene ($R_c^2 = 0.95$).

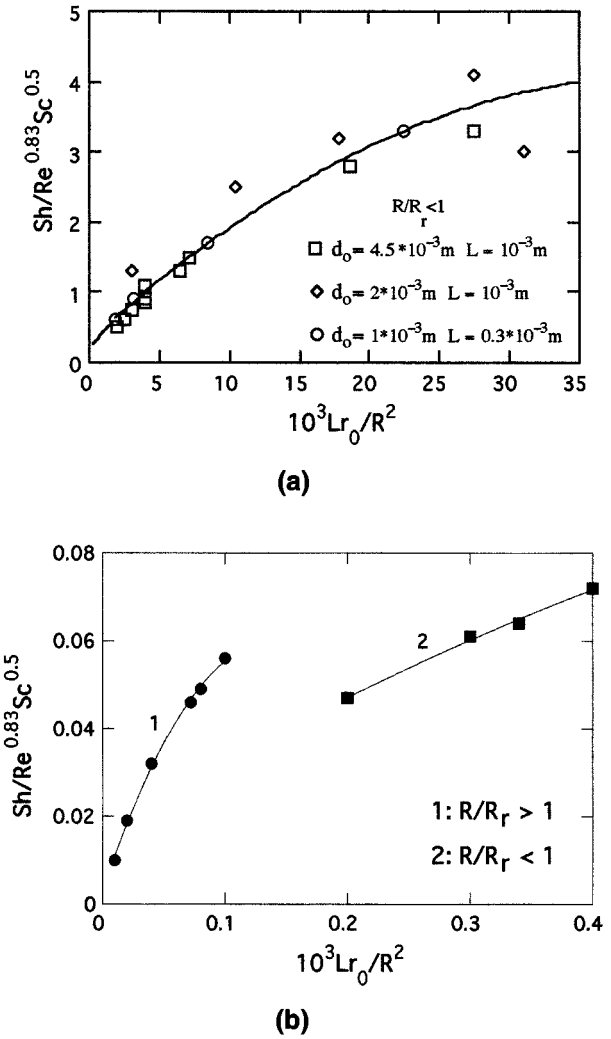

Figure 6. (a) Dependence of dimensionless parameters for water–HCl–water ($R_c^2 = 0.96$); (b) dependence of dimensionless parameters for water–iodine–kerosene ($R_c^2 = 0.99$).

transfer in the film are its velocity u_0 and the radius of the reactors R_r, other quantities remain unchanged. The effect of u_0 and R_r is explored in the following for two operating conditions:

1. $Q_{tot} \sim u_0$, that is, $Q_{tot}/u_0 \sim$ constant, yielding from Eq. 33 that $\varphi \sim (R_r^2)^{-1}$. Thus, it follows from Eqs. 32 and 39 that $k_r \sim u_0^{0.83} R_r^{-1.51}$ and $N_r \sim u_o^{-0.17} R_r^{0.49}$.

2. u_0 is an independent quantity, while $Q_{\text{tot}} = 2\pi r_0 L u_0$ remains constant. Note that in this case r_0 and L can be varied. Thus, $\varphi \sim (r_o R_r^2)^{-1}$, and it follows from Eqs. 32 and 39 that $k_r \sim u_0^{0.16} R_r^{-1.51}$ and $N_r \sim u_0^{0.16} R_r^{0.49}$.

As seen, the values of the mass-transfer coefficient k_r always decrease when the reactor radius R_r increases, probably due to an increase in the boundary layers on the interface between the immiscible films that make up the entire film (Kogan, 1977; Brounshtein and Fishbein, 1977). In addition, considering the variation of N_r vs. u_0, it can be concluded that it is more efficient to operate the present reactor according to the conditions in case 2, which simultaneously will increase the efficiency according to Eqs. 30 and 31.

Power input

Power input (J/m^3) in impinging streams is given by (Tamir, 1994):

$$P = (Q_s \Delta P_s + Q_r \Delta P_r)/(Q_s + Q_r). \tag{40}$$

In the present setup, it was found that for $\gamma \neq 1$, $\Delta P_r \sim \Delta P_r \equiv \Delta P$, probably because the distance between the nozzles was extremely small, of the order of 0.1×10^{-3}m. Thus,

$$P(kJ/m^3) \cong 100 \Delta P(atm). \tag{41}$$

In addition, pressure losses in the nozzles are negligible by comparison to the friction losses due to the 90° change in the flow direction by the liquids leaving the nozzles as well as the small distance between the nozzles (Figure 3). The latter losses are determined as follows. The differential force, df, acting on the liquid while changing its flow trajectory is given by

$$df = \pi r_0^2 d(\Delta P), \tag{42}$$

while the force acting on a mass, m, changing its flow direction (Millikan et al., 1965) reads

$$df = mR_t \beta = \left(\pi r_0^2 u_n \rho \, dt\right) R_t \beta, \tag{43}$$

where $R_t \beta$ is the tangential acceleration of the flow due to its trajectory change. Thus,

$$d(\Delta P) = u_n \rho \beta R_t \, dt. \tag{44}$$

Integration of Eq. 44 between the time the liquid leaves the nozzle, $t = 0$, and the time it enters the film, $t = t_t$, that is, completing its change of flow direction by 90° (see Figure 3), while considering Eq. 44 yields

$$\Delta P = \zeta u_n \rho = \zeta u_o \rho L / r_o, \tag{45}$$

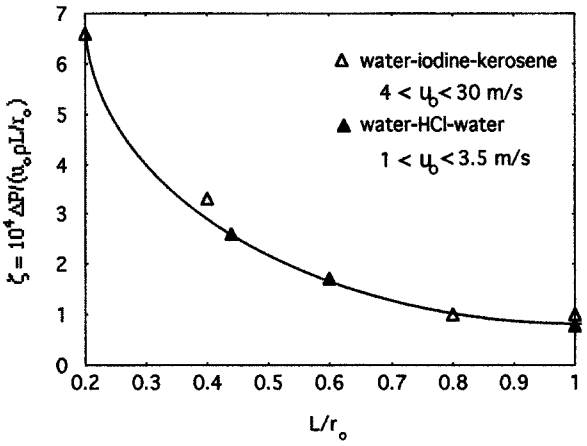

Figure 7. Dimensionless flow resistance vs. initial dimensionless film thickness ($r_c^2 = 0.98$).

Table 3 Regular Extraction Devices* vs. Present Thin-Film Extraction Device

Parameter	Range of data	Regular Devices** Mean Value	Thin-Film Device for $E_{Mr} = 95\%$ Water–Iodine—Kerosene	Water–HCl–Water
k(m/s)	$(1-20)\times10^{-5}$	$\sim 5\times10^{-5}$	0.56×10^{-3}*	9.8×10^{-3}*
K(l/s)	$(0.15-300)\times10^{-4}$	$\sim 35\times10^{-4}$	5.6×10^{-2}*	9.8×10^{-1}*
$t_r(s)$			2×10^{-3}	16×10^{-3}
P(kJ/m^3)	100 – 2,500	$\sim$ 300	280	20
u_0(m/s)			24	2

*Agitated vessels; spray, packed, and perforated-plate columns; disc contractors, rotary and agitated columns (Laddha and Degaleesan, 1976; Treyball, 1963; Tamir, 1994; Perry, 1950; Handlos, 1954); t_r—mean residence time; *—minimal values; k, K—mass-transfer coefficients.

where

$$\zeta\ (\mathrm{m/s}) = \int_0^{t_t} \beta R_t\, dt.$$

It should be emphasized that the determination of ζ is based on experimental data, while Figure 7 demonstrates such results for the present investigation. These data resulted in $\zeta \sim (L/r_o)^{-1.25}$, yielding from Eq. 45 that

$$\Delta P\ (\mathrm{atm}) = A u_o \rho (L/r_o)^{-0.25},$$

where

$$A \approx 0.88\times10^{-4}. \qquad (46)$$

Pressure-loss data are usually expressed via $Eu = f(Re, \zeta_1)$, where ζ_1 is a function of the fluid's trajectory. Defining the following quantities:

$$Re_1 = u_n r_o/\nu \qquad Eu = \Delta P/\rho u_n^2 \qquad \zeta_1 = \zeta r_o/\nu. \qquad (47)$$

where ν is the kinematic viscosity. Thus, for the present investigation Eqs. 45 and 47 yield

$$Eu = \zeta_1/Re_1, \qquad (48)$$

while an equation of the preceding type has been widely used (Elperin, 1972; Tamir, 1994; Kutatelaze and Borishansky, 1959; Povh, 1976).

Conclusions

Table 3 summarizes the major results, that enable one to make comparisons between regular extraction devices and the present device where the extraction process takes place in thin films generated by impinging streams. The major conclusion drawn is that the new device is superior by comparison to other devices, yielding mass-transfer coefficients higher by a factor of 10–200 for a relatively identical power input. In addition, the mean residence time in the new extractor is smaller, which is caused by the relatively fast separation in the settler. This is due to the fact that dispersion between the immiscible films is relatively small; however, mass transfer is intensive, caused by the generation of thin and turbulent films. Preliminary experiments are at present under conduction for cleaning by the new device, phosphoric acid, an important product manufactured by one of the biggest industries in Israel–Rotem Amfert Negev Ltd.

Acknowledgment

The authors acknowledge Mrs. Drora Shmilowitz for conducting the experimental work.

Notation

A = constant in Eqs. 39 and 46
D_i = diffusion coefficient of solute in i, $i = r$ for raffinate, $i = s$ for solvent, m^2/s
E_{Mr}, E_{Me} = extraction efficiencies with respect to raffinate and extract, Eq. 35, %
f = force acting on the fluid while changing its direction by 90°, N
N_r, N_s = dimensionless mass-transfer numbers of the raffinate and solvent, defined by Eqs. 30–32
P = power input, J/m^3
Q_{tot} = total volumetric flow rate of raffinate (feed) and solvent (extract), $Q_{tot} = Q_r + Q_s$, m^3/s
r = coordinate perpendicular to the flow in the nozzle (Figure 3)
r_0 = radius of the nozzle's hole, m
R_2 = radius of curvature of the film of radius R and thickness h, Eq. 8 and see Figure 3, m
$\overline{R}_2$ = mean value of R_2, m
R_t = radius of curvature of the liquid flow while changing flow direction by 90° (Figure 3), m
R_c^2 = correlation coefficient
Re = Reynolds number, defined by Eq. 33
Sc_i = Schmidt number defined in Eq. 33; $i = r$ for raffinate, $i = s$ for solvent
Sh_i = Sherwood number defined in Eq. 33; $i = r$ for raffinate, $i = s$ for solvent
u = local velocity of the liquid in the film, m/s
u_0 = initial mean velocity of the liquids in the film defined by $Q_{tot} = Q_r + Q_s = 2\pi r_0 L u_0$, m/s
u_n = mean velocity of the phases inside the nozzle, m/s
V_r = volume of the reactor, $\pi R^2 H$, m^3
x_1, x_2 = initial and final concentrations of solute in raffinate, mg/(cm^3 raffinate)
x_1^*, x_2^* = initial and final equilibrium concentrations of solute in raffinate corresponding to y_1 and y_2, respectively, mg/(m^3 raffinate)
y_1, y_2 = initial and final concentrations of solute in solvent, mg/(cm^3 solvent)
y_1^*, y_2^* = initial and final equilibrium concentrations of solute in the solvent corresponding to x_1 and x_2, respectively mg/(cm^3 solvent)
β = angular acceleration of a liquid while changing direction along its trajectory, rad/s^2
δ' = coordinate at initial film thickness perpendicular to the film flow, see Figure 3

ΔP = pressure drop on solvent and raffinate streams, N/m^2
ρ = mean density of the liquid phases, kg/m^3
ζ = proportionality coefficient in Eq. 45, m/s
φ = dimensionless geometrical factor or ratio between flow rates, defined in Eq. 33

Literature Cited

Angelov, G., C. Gourdon, and A. Line, "Simulation of Flow Hydrodynamics in a Pulsed Solvent Extraction Column Under Turbulent Regime," *Chem. Eng. J.*, **71**, 1 (1998).

Bouaifi, M., and M. Roustan, "Bubble Size and Mass Transfer Coefficients in Dual Impeller Agitated Reactors," *Can. J. Chem. Eng.*, **76**, 390 (1998).

Boyadjiev, C., and Y. Beshkov, *Mass Transfer in Liquid Film Flow*, The Academy of Sciences, Bulgary, Sofia, (1984).

Brounshtein, B. J., and G. A. Fishbein, *Hydrodynamic, Mass and Heat Transfer in the Dispersion Systems*, (in Russian), Publisher Chemistry USSR, Leningrad (1977).

Carver, J. A., S. Plains, and W. F. Rollman, "Method and Apparatus for Mixing and Contacting Fluids," U.S. Patent No. 2,751,335 (June 19, 1956).

Chu, K. J., and A. E. Dukler, "Statistical Characteristics of Thin Wavy Films," *AIChE J.*, **20**, 695 (1974).

Czapla, C., and H. J. Bart, "Acetic Acid Extraction Under the Influence of Chemical Absorption Layers," *Int. Congr. of Chemical and Process Engineering, Czech Republic*, Process Engineering Publisher, Praha, p. 9 (1998).

Davies, J. T., "Turbulence Phenomena at Free Surfaces," *AIChE J.*, **18**, 169 (1972).

Eckert, R. G., and R. M. Drake, *Theory Heat and Mass Transfer* (in Russian), Energy Publishing USSR, Moscow (1961).

Elperin, I. T., *Transport Processes in Impinging Jets*, (in Russian), Science and Technique, Minsk, USSR, (1972).

Handlos, A. E., and T. Baron, "Mass and Heat Transfer from Drops in Liquid-Liquid Extraction," *AIChE J.*, **3**, 127 (1957).

Hasson, D., and R. E. Peck, "Thickness Distribution in a Sheet Formed by Impinging Jets," *AIChE J.*, **10**, 752 (1964).

Janssen, J. M. H., G. W. M. Peters, and H. E. H. Meijer, "An Opposed Jet Device for Studying the Breakup of Dispersed Liquid Drops," *Chem. Eng. Sci.*, **48**, 255 (1993).

Kapiza, P. L, "Wavy Motion of the Thin Liquid Layers," (in Russian), *J. Exp. Theory. Phys.*, **48**, 1 (1948).

Kogan, V. B., *Theoretical Principles of the Basic Processes in the Chemical Technology*, (in Russian), Publisher Chemistry USSR, Leningrad (1977).

Korn, G. K., and T. M. Korn, *Mathematical Handbook*, McGraw-Hill, New York (1968).

Kutatelaze, S. S., and V. M. Borishansky, *Handbook of the Heat Transfer*, (in Russian), Energy Published USSR, Moscow (1959).

Laddha, G. S., and T. E. Degaleesan, *Transport Phenomena in Liquid Extraction*, McGraw-Hill, New Delhi (1976).

Manzurela, E., *Analytical Chemistry*, Kavim, Israel (1997).

Marchuk, J. C., "Experimental Study of Dispersions and Separation of Phases in Liquid-Liquid Extraction of Copper by LJX64N in Various Types of Mixers," *Ind. Eng. Chem. Process Des. Dev.*, **19**, 522 (1980).

McKetta, J. J., ed., *Encyclopedia of Chemical Processing and Design*, Vol. 14, Marcel Dekker, New York, p. 718 (1984).

Millikan, R. A., D. Roller, and E. C. Watson, *Mechanics, Molecular, Physics, Heat and Sound*, M.I.T. Press, Cambridge, MA (1965).

Misek, T., "Recommended Systems for Liquid Extraction Studies," European Federation of Chemical Engineers, Rugby, Warwickshire, U.K. (1987).

Perry, H., *Chemical Engineer's Handbook*, McGraw-Hill, New York (1950).

Popiel, C. P., and O. Trass, "Visualization of a Free and Impinging Round Jet," *Exp. Therm. Fluid Sci.*, **4**, 253 (1991).

Povh, J. L., *Technical Hydrodynamics*, (in Russian), Mechanical Engineering, Publishing, Leningrad (1976).

Ranz, W. E., "Some Experiments on the Dynamics of Liquid Films," *J. App. Phys.*, **30**, 1950 (1959).

Rauline, D., P. A. Tanguy, J. Le Blevec, and J. Bousquet, "Numerical Investigation of the Performance of Several Static Mixers," *Can. J. Chem. Eng.*, **53** 527 (1998).

Reid, R. C., J. M. Prausnitz, and B. E.Pauling, *The Properties of Gases and Liquids*, McGraw-Hill, New York (1987).

Rydberg, Y., C. Musikas, and G. R. Choppin, *Principles and Practices of Solvent Extraction*, Dekker, New York (1992).

Tamir, A., *Impinging-Stream Reactors*: *Fundamentals* & *Applications*, Elsevier, Amsterdam (1994).

Taylor, G., "Formation of Thin Flat Sheets of Water," *Proc. Roy. Soc.*, **259**, 1 (1960).

Treyball, R. E., *Liquid Extraction*, McGraw-Hill, New York (1963).

Weigl, B. H., and P. Yager, "Microfluidic Diffusion-Based Separation and Detection," *Science*, **283**, 346 (1999).

Wilson, S., and V. Manousiouthakis, "Minimum Utility Cost for a Multicomponent Mass Exchange Operation," *Chem. Eng. Sci.*, **53**, 3887 (1998).

Manuscript received July 14, 1999, and revision received Nov. 15, 1999.